

$B \rightarrow K\nu\bar{\nu}$, MiniBooNE and muon $g - 2$ anomalies from a dark sector

Alakabha Datta,^{1, 2, 3,*} Danny Marfatia,^{4, †} and Lopamudra Mukherjee^{5, ‡}

¹*Department of Physics and Astronomy, University of Mississippi, 108 Lewis Hall, Oxford, MS 38677, USA*

²*SLAC National Accelerator Laboratory, 2575 Sand Hill Road, Menlo Park, CA 94025, USA*

³*Santa Cruz Institute for Particle Physics, Santa Cruz, CA 95064, USA*

⁴*Department of Physics and Astronomy, University of Hawaii, Honolulu, HI 96822, USA*

⁵*School of Physics, Nankai University, Tianjin 300071, China*

Belle II has reported the first evidence for $B^+ \rightarrow K^+\nu\bar{\nu}$ with a branching ratio 2.7σ higher than the standard model expectation. We explain this, and the MiniBooNE and muon anomalous magnetic moment anomalies in a model with a dark scalar that couples to a slightly heavier sterile Dirac neutrino and that communicates with the visible sector via a Higgs portal. We make predictions for rare kaon and other B meson decays.

Introduction. Anomalies in the charged and neutral current B decays have been an active area of research for almost a decade. The recently updated measured values of $R_{K^{(*)}} = \mathcal{B}(B \rightarrow K^{(*)}\mu^+\mu^-)/\mathcal{B}(B \rightarrow K^{(*)}e^+e^-)$ are now fully consistent with the standard model (SM) expectation [1], and have dampened interest in neutral current (NC) B anomalies (although the individual branching fractions remain discrepant [2]). However, a first measurement by Belle II of the branching ratio $\mathcal{B}(B^+ \rightarrow K^+\nu\bar{\nu}) = (2.3 \pm 0.7) \times 10^{-5}$ [3], is 2.7σ higher than the SM expectation $\mathcal{B}(B^+ \rightarrow K^+\nu\bar{\nu})_{\text{SM}} = (5.58 \pm 0.38) \times 10^{-6}$ [4], and has revived interest in NC B decays [5–10]; an earlier upper limit by Belle II [11] also led to a flurry of theoretical activity [12–17]. Unlike the dilepton modes in $R_{K^{(*)}}$, the contamination from $c\bar{c}$ states in $B \rightarrow K^{(*)}\nu\bar{\nu}$ can be neglected. Hence, if confirmed, the Belle II result could be a clear sign of new physics. Note that any theoretical interpretation must be compatible with constraints on the other $B \rightarrow K^*\nu\bar{\nu}$ decays in Table I.

Decays of B mesons that involve invisible final states are excellent probes of new invisible or long lived states like a massive sterile neutrino, ν_D . These states may be produced via mixing with the active neutrinos or through new mediators such as new vector bosons or leptoquarks that couple them to SM particles. We consider a mechanism in which ν_D communicates with the SM sector through a light scalar mediator S [18] which couples to the SM sector through an extended Higgs portal [19–21]. The scalar couples to active neutrinos via four-neutrino mixing and a contribution to $B^+ \rightarrow K^+\nu\bar{\nu}$ is generated by the two body decays, $B^+ \rightarrow K^+S$ and $S \rightarrow \nu\bar{\nu}$.

Our framework also permits an understanding of the excess in electron like events in the MiniBoone experi-

ment [22] in terms of a light neutrino upscattering into ν_D which subsequently decays to $\nu S(\rightarrow e^+e^-, \gamma\gamma)$. Note that similar upscattering into ν_D via a dark vector boson Z' [23, 24] is excluded [25] by data from the CHARM-II [26] and MINERVA [27] experiments if the Z' is lighter than the sterile neutrino as in Ref. [23]. As shown in Ref. [18], with a light scalar mediator, the solution to the MiniBooNE anomaly is consistent with the CHARM-II and MINERVA data even with S lighter than the sterile neutrino. It is noteworthy that this explanation is untested by the template analysis of MicroBooNE [28].

Another long-standing anomaly is that of the anomalous magnetic moment of the muon, $a_\mu \equiv (g - 2)_\mu/2$. The SM prediction [29] is more than 5σ smaller than the updated world average following the latest experimental measurement [30]:

$$\Delta a_\mu = a_\mu^{\text{exp}} - a_\mu^{\text{SM}} = (2.49 \pm 0.48) \times 10^{-9}. \quad (1)$$

The anomaly can be resolved by including a higher dimensional coupling to two photons [18, 20]. This coupling can also help explain the MiniBooNE anomaly because it enables the scalar to decay to photon pairs which can be misidentified as electron events at MiniBooNE.

Model. The scalar Lagrangian is given by

$$\begin{aligned} \mathcal{L}_S &\supset \frac{1}{2}(\partial_\mu S)^2 - \frac{1}{2}m_S^2 S^2 - \eta_d \sum_{f=d,\ell} \frac{m_f}{v} \bar{f} f S \\ &\quad - \sum_{f=u,c,t} \eta_f \frac{m_f}{v} \bar{f} f S - g_D S \bar{\nu}_D \nu_D - \frac{1}{4} \kappa S F_{\mu\nu} F^{\mu\nu}, \end{aligned} \quad (2)$$

where $v \simeq 246$ GeV, is the Higgs vacuum expectation value, d and ℓ correspond to down-type quarks and leptons with a universal coupling η_d scaled by the respective SM Yukawa. The structure of the Lagrangian can arise from the mixing of singlet scalar with the neutral components of a two Higgs doublet model [19–21]. We will however adopt an effective interaction in the spirit of Ref. [18] and

* datta@phy.olemiss.edu

† dmarf8@hawaii.edu

‡ lopamudra.physics@gmail.com

| Observable | SM expectation | Measurement or constraint |
|---|--|---|
| $\mathcal{B}(B^+ \rightarrow K^+ \nu \bar{\nu})$ | $(5.58 \pm 0.38) \times 10^{-6}$ [4] | $(2.3 \pm 0.7) \times 10^{-5}$ [3] |
| $\mathcal{B}(B^0 \rightarrow K^{*0} \nu \bar{\nu})$ | $(9.2 \pm 1.0) \times 10^{-6}$ [33] | $< 1.8 \times 10^{-5}$ [34] |
| $\mathcal{B}(B^+ \rightarrow K^{*+} \nu \bar{\nu})$ | $\mathcal{B}(B^0 \rightarrow K^{*0} \nu \bar{\nu}) \frac{f_{B^+}}{f_{B^0}}$ [33] | $< 4 \times 10^{-5}$ [35] |
| $\mathcal{B}(B^0 \rightarrow K^{*0} e^+ e^-)_{m_{e^+ e^-} \geq 140 \text{ MeV}}$ | $(2.43^{+0.66}_{-0.47}) \times 10^{-7}$ [36] | $(3.1^{+0.9+0.2}_{-0.8-0.3} \pm 0.2) \times 10^{-7}$ [37] |
| $\mathcal{B}(B_s \rightarrow \gamma \gamma)$ | 5×10^{-7} [38] | $< 3.1 \times 10^{-6}$ [39] |
| $\mathcal{B}(B_s \rightarrow \mu^+ \mu^-)$ | $(3.57 \pm 0.17) \times 10^{-9}$ [40] | $(3.52^{+0.32}_{-0.31}) \times 10^{-9}$ [41] |
| $\mathcal{B}(K_L \rightarrow \pi^0 \nu \bar{\nu})$ | $(3.4 \pm 0.6) \times 10^{-11}$ [42] | $< 4.9 \times 10^{-9}$ [43] |
| $\mathcal{B}(K_L \rightarrow \pi^0 e^+ e^-)$ | $(3.2^{+1.2}_{-0.8}) \times 10^{-11}$ [44] | $< 2.8 \times 10^{-10}$ [45] |
| $\mathcal{B}(K_L \rightarrow \pi^0 \gamma \gamma)$ | - | $(1.273 \pm 0.033) \times 10^{-6}$ [46] |
| $\mathcal{B}(K_S \rightarrow \pi^0 \gamma \gamma)$ | - | $(4.9 \pm 1.8) \times 10^{-8}$ [46] |
| $\mathcal{B}(K^+ \rightarrow \pi^+ \gamma \gamma)$ | - | $(1.01 \pm 0.06) \times 10^{-6}$ [46] |
| $\mathcal{B}(K^\pm \rightarrow \mu^\pm \nu_\mu e^+ e^-)_{m_{e^+ e^-} \geq 140 \text{ MeV}}$ | - | $(7.81 \pm 0.23) \times 10^{-8}$ [47] |
| ΔM_{B_s} | $(18.4^{+0.7}_{-1.2}) \text{ ps}^{-1}$ [48] | $(17.765 \pm 0.006) \text{ ps}^{-1}$ [46] |
| ΔM_K | $(47 \pm 18) \times 10^8 \text{ s}^{-1}$ [49] | $(52.93 \pm 0.09) \times 10^8 \text{ s}^{-1}$ [46] |
| a_μ | $116591810(43) \times 10^{-11}$ [29] | $116592059(22) \times 10^{-11}$ [30] |

TABLE I. Experimental measurements and constraints used in the analysis. The upper limits are at 90% C.L.

take the couplings η_f of the scalar to the up-type quarks to not be flavor universal. The parameter κ , of inverse mass dimension, induces an $S\gamma\gamma$ coupling which contributes to $(g-2)_\mu$ via the one-loop Barr-Zee diagram [31]. (Without this higher dimensional operator, the contributions to $(g-2)_\mu$ are via the vertex correction of the $\gamma\mu^+\mu^-$ vertex and self-energy diagrams which are insufficient to address the anomaly [20].)

The light active neutrinos mix with the heavy sterile neutrino and induce a coupling of the dark scalar to the light neutrinos. The four flavor eigenstates ν_α are related to the mass eigenstates ν_i by

$$\nu_{\alpha(L,R)} = \sum_{i=1}^4 U_{\alpha i} \nu_{i(L,R)}, \quad \alpha = e, \mu, \tau, D, \quad (3)$$

where L, R indicate the handedness of the neutrino, and U is a 4×4 orthogonal matrix common to ν_L and ν_R . We take $U_{e4} = U_{\tau 4} = 0$ which gives $1 - |U_{D4}|^2 = |U_{\mu 4}|^2$ by unitarity. We require ν_4 to be a Dirac neutrino so that its nonrelativistic decays, $\nu_4 \rightarrow \nu S$, are not isotropic [32], as required by MiniBooNE data. Note that the sterile neutrino will have a much shorter lifetime $\sim |U_{\mu 4}|^{-2}$ than the scalar $\sim |U_{\mu 4}|^{-4}$.

The coupling of the light scalar to up-type quarks and light neutrinos yields several flavor changing neutral current transitions via the penguin loop. The rare hadronic decays in Table I provide constraints on the model.

Signals and constraints. We consider a dark scalar with mass in the range $10 \lesssim m_S/\text{MeV} \lesssim 150$. Since $m_S < 2m_\mu$, S can only decay to photons, electrons and neutrinos, for which the decay widths are provided in the Supplemental Material. Below, we discuss the phenomenological implications for several observables of interest and the constraints imposed on the model.

S decay length. We require the decay length of the dark scalar to be shorter than 0.1 mm to evade bounds from

beam dump and other experiments that probe long-lived particles.

B and K meson decays. The Lagrangian in Eq. (2) induces two-body meson decays such as $B \rightarrow K^{(*)}S$ and $K \rightarrow \pi S$ at one loop. The flavor changing neutral current (FCNC) Lagrangian for the $b \rightarrow s$ and $s \rightarrow d$ transitions is given by

$$\mathcal{L}_{\text{FCNC}} = g_{bs} \bar{s} P_R b S + g_{sd} \bar{d} P_R s S, \quad (4)$$

where the effective couplings g_{bs}, g_{sd} take the form,

$$g_{bs} \approx \frac{3\sqrt{2}G_F}{16\pi^2} \frac{m_t^2 m_b}{v} \eta_t V_{tb} V_{ts}^*, \quad (5)$$

and

$$g_{sd} \approx \frac{3\sqrt{2}G_F}{16\pi^2} \frac{m_t^2 m_s}{v} V_{ts} V_{td}^* \left(\eta_t + \eta_c \frac{m_c^2}{m_t^2} \frac{V_{cs} V_{cd}^*}{V_{ts} V_{td}^*} \right). \quad (6)$$

The rates for the two body FCNC processes can be found in the Supplemental Material. The relevant B meson form factors are taken from Refs. [50, 51] while the kaon form factor $|f_0^K(m_S^2)|^2$ is approximately unity [52]. It is important to note that g_{bs} is essentially determined by η_t since the contribution proportional to η_c is both helicity and charm-mass suppressed. On the other hand, for g_{sd} , the contribution from η_c is only helicity suppressed and can be sizable for $\eta_c \gg \eta_t$. $\mathcal{L}_{\text{FCNC}}$ also induces B_s decays to $\gamma\gamma, \mu^+\mu^-$ and $\nu\bar{\nu}$. The most important constraints on the couplings from the flavor changing B and K transitions are as follows:

1. *B decay width:* We require $\mathcal{B}(B \rightarrow K^{(*)}S) < 10\%$ so that it does not exceed the uncertainty in the SM prediction of the B meson width [53].
2. *B $\rightarrow K\nu\bar{\nu}$:* We require $\mathcal{B}(B^+ \rightarrow K^+ \nu\bar{\nu})$ to lie within 1σ of the Belle II measurement in the first row of Table I.
3. *B $\rightarrow K^* \nu\bar{\nu}$:* We ensure that the upper limits on the branching fractions of the $B \rightarrow K^*$ modes in Table I are satisfied.
4. *B $^0 \rightarrow K^{*0} e^+ e^-$:* This decay has been measured by LHCb in the low dilepton mass region of 30-1000 MeV/c 2 [37] which overlaps the mass range of the dark scalar. We therefore require the branching ratio to lie within 1σ of the measured value.
5. *B $_s$ decays:* We require the scalar contribution to $B_s \rightarrow \gamma\gamma$ to remain below the upper limit placed by Belle [39] and the contribution to $B_s \rightarrow \mu^+\mu^-$ to remain within the 1σ uncertainty of the measurement in Table I. We take the decay constant $f_{B_s} = 230.3(1.3)\text{MeV}$ from Ref. [54]. An interesting signature is $B_s \rightarrow$ invisible which is currently not constrained by experiment but can be probed at Belle II. We make predictions for its branching fraction for some benchmark points.

6. $K^+ \rightarrow \pi^+ \nu \bar{\nu}$: The NA62 experiment at CERN has set stringent limits on $\mathcal{B}(K^+ \rightarrow \pi^+ X)$ as a function of the X mass and lifetime for invisible X decays except in the range $110 < m_X/\text{MeV} < 160$ [55, 56]. However, since S has a very short lifetime, $\mathcal{O}(0.1)$ ps, these limits do not apply.
7. $K_L \rightarrow \pi^0 \nu \bar{\nu}$: We require that the most recent upper limit on the branching fraction from the KOTO experiment at J-PARK be satisfied; see Table I.
8. $K \rightarrow \pi \gamma \gamma$: For these decay modes, we require the dark scalar contribution to be smaller than the measured central values in Table I.
9. $K^\pm \rightarrow \mu^\pm \nu_\mu e^+ e^-$: The NA48/2 Collaboration has measured $\mathcal{B}(K^\pm \rightarrow \mu^\pm \nu_\mu e^+ e^-) = (7.81 \pm 0.23) \times 10^{-8}$ [47] in the kinematic region $m_{e^+ e^-} \geq 140$ MeV. In our model this decay proceeds through $K \rightarrow \mu \nu S (\rightarrow e^+ e^-)$ where the dark scalar is radiated off the muon leg. The constraint applies for $m_S > 140$ MeV.

B and K meson mixing. The Lagrangian in Eq. (4) also induces meson mixing. The measurement of the mass difference ΔM_{B_s} is consistent with the SM prediction. Hence we require the additional contribution to not exceed the uncertainty in the SM expectation. For kaon mixing, the SM prediction suffers from large uncertainties. The long distance contribution is poorly estimated, so we only include the short distance contribution to ΔM_K in Table I. The measured value, however, is quite precise and we do not allow the new contribution to ΔM_K to exceed the 1σ uncertainty in the measurement.

$(g-2)_\ell$. The dominant contribution to the anomalous magnetic moments of the muon and electron comes from the log enhanced term of the Barr-Zee diagram (see Supplemental Material) which depends on the cut-off scale Λ . We fix $\Lambda = 2$ TeV and require consistency with Eq. (1) within 1σ . Because $\Delta a_e / \Delta a_\mu = m_e^2 / m_\mu^2$, we find $\Delta a_e \sim \text{few} \times 10^{-14}$ which is much smaller than the magnitude of the inferred value, $\mathcal{O}(10^{-13} - 10^{-12})$ [57–59].

MiniBooNE. The scattering of a muon neutrino off a nucleus may take place via the dark scalar exchange as shown in Fig. 1. Being heavy, the sterile neutrino produced promptly decays to a light neutrino and the dark scalar, whose subsequent decay to $e^+ e^-$ and $\gamma\gamma$ may mimic the signal observed in the MiniBooNE experiment. Since MiniBooNE is a Cherenkov detector that cannot distinguish between electrons and photons, two photons or two electrons with a small opening angle can be misidentified as a single electron. The details of the coherent scattering cross sections mediated by the dark scalar can be found in the Supplemental material.

It has been previously shown in Ref. [18] that the dark scalar model is able to explain the excess observed in MiniBooNE data while being consistent with the observations of the CHARM II experiment for m_{ν_4} between 400 MeV and 500 MeV. The sterile neutrino has to be heavier than 400 MeV to ensure that less than 70% of the excess events

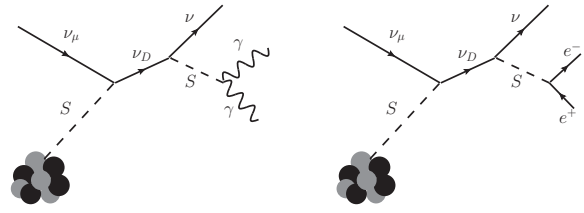


FIG. 1. Dark scalar mediated neutrino-nucleus scattering produces the MiniBooNE signal.

are in the forward most bin ($0.8 < \cos \theta < 1$) of the angular distribution of electron-like events at MiniBooNE [25]. We compute the coherent and incoherent scattering cross sections at MiniBooNE and CHARM-II and recast the results of Refs. [23, 25] for a dark Z' kinetically mixed with the electromagnetic field, to our case. The following constraints are imposed to implement the mapping between the dark Z' model and our model:

1. In terms of the total scattering cross sections σ_S and $\sigma_{Z'}$ for the scalar and Z' mediators, respectively, we define,

$$\mathcal{R} = \frac{\int \Phi \frac{d\sigma_S}{dT} dT dE_{\nu_\mu} \times (\mathcal{B}(S \rightarrow e^+ e^-) + \mathcal{B}(S \rightarrow \gamma\gamma))}{\int \Phi \frac{d\sigma_{Z'}}{dT} dT dE_{\nu_\mu} \times \mathcal{B}(Z' \rightarrow e^+ e^-)}, \quad (7)$$

with the denominator evaluated at the benchmark point $m_{Z'} = 30$ MeV, $\alpha_{Z'} = 0.25$, $\alpha e^2 = 2 \times 10^{-10}$ of Ref. [23] to explain the MiniBooNE anomaly. The ν_μ flux at the Booster Neutrino Beam in the neutrino run [22] is denoted by Φ . To reproduce the MiniBooNE signal we require $0.95 \leq \mathcal{R} \leq 1.05$.

2. The Z' model of Ref. [23], however, is excluded by the CHARM-II constraint in Ref. [25]. To satisfy this constraint we require

$$\frac{\sigma_S \times (\mathcal{B}(S \rightarrow e^+ e^-) + \mathcal{B}(S \rightarrow \gamma\gamma))}{\sigma_{Z'} \times \mathcal{B}(Z' \rightarrow e^+ e^-)} < 1 \quad (8)$$

for $E_{\nu_\mu} = 20$ GeV, where the denominator is evaluated for the parameter values in Fig. 3 of Ref. [25] with $|U_{\mu 4}| = 10^{-4}$.

Heavy neutral lepton searches. Several experiments including PS191 [60], NuTeV [61], BEBC [62], FMMF [63], CHARM II [64], T2K [65], NA62 [66] and MicroBooNE [67] have placed limits on heavy neutral leptons with sufficiently long lifetimes that can reach the detector before decaying into SM particles. However, the limits on $U_{\mu 4}$ from the nonobservation of the decay signal do not apply to our model because ν_4 has a lifetime of $\mathcal{O}(0.1)$ ps and decays promptly. The only relevant bound for m_{ν_4} between 400 MeV and 700 MeV arises from lepton universality: $|U_{\mu 4}| \lesssim 0.07$ at the 99% C.L. [68].

Analysis and results. We analyze two cases: $\kappa \neq 0$ and $\kappa = 0$. We find that $\eta_t \gtrsim 0.005$ is needed to explain the measured branching fraction of $B^+ \rightarrow K^+ \nu \bar{\nu}$.

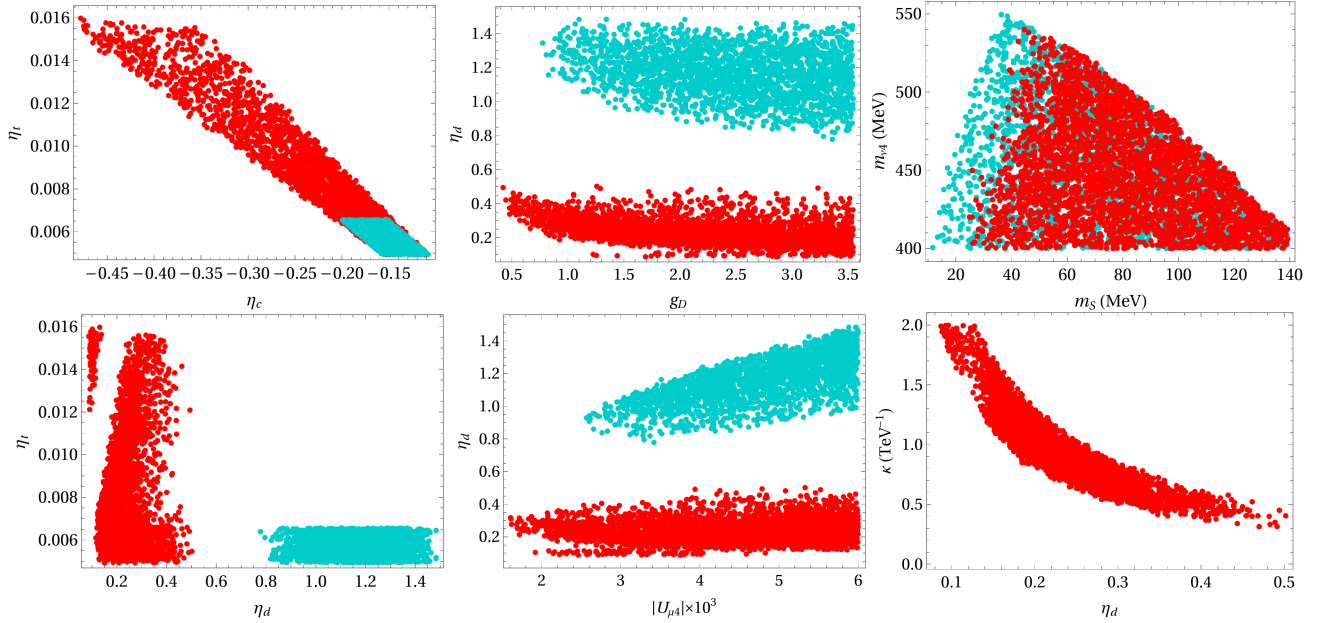


FIG. 2. Allowed regions depicted by red points for $\kappa \neq 0$ and cyan for $\kappa = 0$.

However, this leads to a correction to the $K_L \rightarrow \pi^0 \nu \bar{\nu}$ branching fraction that violates the upper limit set by the KOTO experiment. To lower the new contribution to $K_L \rightarrow \pi^0 \nu \bar{\nu}$, a cancellation between the η_t and η_c dependent terms in g_{sd} is required. This is achieved for $\eta_c \approx -27\eta_t$. The large η_c does not, however, affect g_{bs} significantly due to the charm mass suppression. If nonzero, the coupling κ is primarily constrained by MiniBooNE and $g - 2$ data. Even though the FCNC transitions to invisible final states depend upon the sterile neutrino parameters g_D and $U_{\mu 4}$, these are mainly constrained by the ν_μ -nucleus scattering cross section. For $\kappa \neq 0$ and $\kappa = 0$, we set $\eta_u = 0$ for simplicity and scan the other parameters in the following ranges:

$$\begin{aligned} \eta_d &\in [0, 1], \quad \eta_t \in [0, 0.02], \quad \eta_c \in [-0.5, 0], \\ g_D &\in [0, \sqrt{4\pi}], \quad \kappa \in [0, 2] \text{ TeV}^{-1}, \quad |U_{\mu 4}| \in [0, 0.006], \\ m_S &\in [10, 150] \text{ MeV}, \quad m_{\nu 4} \in [400, 700] \text{ MeV}. \end{aligned}$$

For both cases, we choose some benchmark points (BPs) that have interesting consequences for rare K and B decays.

a. $\kappa \neq 0$: In this case, the dark scalar has a nonzero effective coupling to photons which permits an explanation of the discrepancy in the muon anomalous magnetic moment. The MiniBooNE signal is also enhanced due to the nonzero branching fraction to $\gamma\gamma$. In Fig. 2, we show the allowed regions by the red points. As explained above, there is a strong correlation between η_t and η_c . A significant correlation is also observed between m_S and $m_{\nu 4}$. For certain values of η_d , the effective scalar-nucleus coupling responsible for neutrino-nucleus scattering becomes too small to produce a significant scattering cross

| BP | κ (TeV $^{-1}$) | η_d | η_c | $\eta_t \times 10^2$ | g_D | $U_{\mu 4} \times 10^3$ | m_S (MeV) | $m_{\nu 4}$ (MeV) |
|----|-------------------------|----------|----------|----------------------|-------|-------------------------|-------------|-------------------|
| 1 | 1.22 | 0.17 | -0.13 | 0.54 | 2.18 | 4.86 | 38 | 413 |
| 2 | 0.60 | 0.30 | -0.28 | 1.04 | 0.94 | 3.64 | 93 | 413 |
| 3 | 1.21 | 0.21 | -0.24 | 0.84 | 1.26 | 5.65 | 93 | 432 |
| 4 | 1.03 | 0.20 | -0.14 | 0.58 | 3.42 | 3.25 | 44 | 514 |
| 5 | 0.54 | 0.44 | -0.34 | 1.31 | 0.52 | 4.82 | 138 | 404 |
| 6 | 0 | 0.88 | -0.13 | 0.54 | 3.06 | 4.73 | 24 | 401 |
| 7 | 0 | 1.40 | -0.15 | 0.63 | 1.82 | 5.87 | 122 | 429 |

TABLE II. Benchmark points for $\kappa \neq 0$ and $\kappa = 0$ (in which case the $g - 2$ anomaly is unsolved).

| BP | $\mathcal{B}(S \rightarrow \gamma\gamma)$ | $\mathcal{B}(S \rightarrow \nu \bar{\nu})$ | $\mathcal{B}(S \rightarrow e^+ e^-)$ | $\mathcal{B}(K_L \rightarrow \pi^0 \nu \bar{\nu})$ | $\mathcal{B}(B_s \rightarrow \nu \bar{\nu})$ | $\mathcal{B}(B \rightarrow K^{(*)}\gamma\gamma)$ |
|----|---|--|--------------------------------------|--|--|--|
| 1 | 0.093 | 0.907 | 4.26×10^{-5} | 1.71×10^{-9} | 5.13×10^{-7} | 1.3×10^{-6} |
| 2 | 0.717 | 0.282 | 7.06×10^{-4} | 3.61×10^{-11} | 3.54×10^{-7} | 3.7×10^{-5} |
| 3 | 0.496 | 0.504 | 5.93×10^{-5} | 9.02×10^{-10} | 4.14×10^{-7} | 1.7×10^{-5} |
| 4 | 0.165 | 0.835 | 1.10×10^{-4} | 1.73×10^{-9} | 1.43×10^{-6} | 2.65×10^{-6} |
| 5 | 0.829 | 0.170 | 9.72×10^{-4} | 2.04×10^{-10} | 1.72×10^{-7} | 6.8×10^{-5} |
| 6 | 4.58×10^{-6} | 0.999 | 7.10×10^{-4} | 1.89×10^{-9} | 1.01×10^{-6} | 6.5×10^{-11} |
| 7 | 3.95×10^{-4} | 0.997 | 2.14×10^{-3} | 2.84×10^{-9} | 4.86×10^{-7} | 7.6×10^{-9} |

TABLE III. Predictions for the benchmark points in Table II.

section due to the fine-tuning between η_t and η_c . Hence we observe gaps in the allowed regions of η_d .

We select five benchmark points, as listed in Table II, that simultaneously explain the $B^+ \rightarrow K^+ \nu \bar{\nu}$, MiniBooNE and $g - 2$ anomalies. For each BP we also provide predictions for some important decays in Table III.

b. $\kappa = 0$: The allowed regions are shown by the cyan points in Fig. 2. Since the branching of $S \rightarrow \nu \bar{\nu}$ is enhanced in the absence of the $\gamma\gamma$ mode, η_t is restricted

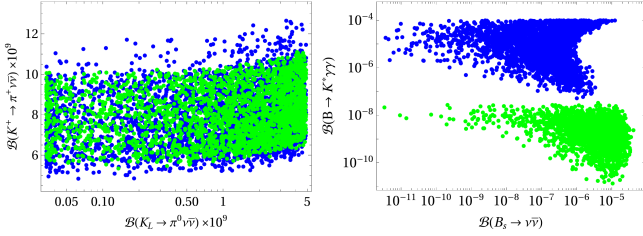


FIG. 3. Branching fractions for kaon and B meson decays for $\kappa \neq 0$ (blue) and $\kappa = 0$ (green).

to smaller values by $\mathcal{B}(B \rightarrow K^{(*)}\nu\bar{\nu})$. The correlation of η_t with η_c remains the same as in the previous case. Further, the contribution to the MiniBooNE signal now only arises from the decay of the dark scalar to e^+e^- . Hence, larger values of η_d are required to enhance the overall coherent scattering cross section. Smaller values of g_D and the mixing parameter $U_{\mu 4}$ are also disfavored. Two benchmark points and predictions for them are provided in Tables II and III, respectively.

Correlations between the branching fractions for kaon and B meson decays are shown in Fig. 3. The branching fraction for $K^+ \rightarrow \pi^+\nu\bar{\nu}$ is predicted to lie in a quite narrow range. Note that $K^+ \rightarrow \pi^+\nu\bar{\nu}$ and $B_s \rightarrow \nu\bar{\nu}$ are

currently unconstrained for a short-lived dark scalar and sterile neutrino.

Summary. Motivated by the recent Belle II evidence for $B^+ \rightarrow K^+\nu\bar{\nu}$ which shows a $\sim 3\sigma$ excess relative to the SM prediction, we explored a new physics explanation of the result in terms of new light states. The new physics contribution to this decay is interpreted as $B^+ \rightarrow K^+S$, where S is a light scalar in the mass range $10 \lesssim m_S/\text{MeV} \lesssim 140$ which then decays to light neutrinos. The interaction of S with light neutrinos occurs via its coupling to a heavy neutral lepton ν_D which mixes with the light neutrinos. We demonstrated that our model is consistent with other measurements and bounds and has interesting predictions for several B and K decays. The excess in electron-like events observed by the MiniBooNE experiment is explained by the upscattering of ν_μ to ν_D which subsequently decays to e^+e^- and $\gamma\gamma$ states. Finally, our model can accommodate the recent muon $g-2$ measurement if S directly couples to photons.

Acknowledgments. A.D. thanks the SLAC National Accelerator Laboratory and the Santa Cruz Institute of Particle Physics for their hospitality during the completion of this work. A.D. is supported in part by the U.S. National Science Foundation under Grant No. PHY-2309937 D.M. is supported in part by the U.S. Department of Energy under Grant No. de-sc0010504.

-
- [1] R. Aaij *et al.* (LHCb), Phys. Rev. Lett. **131**, 051803 (2023), arXiv:2212.09152 [hep-ex].
 - [2] B. Capdevila, A. Crivellin, and J. Matias, (2023), arXiv:2309.01311 [hep-ph].
 - [3] I. Adachi *et al.* (Belle-II), (2023), arXiv:2311.14647 [hep-ex].
 - [4] W. G. Parrott, C. Bouchard, and C. T. H. Davies (HPQCD), Phys. Rev. D **107**, 014511 (2023), [Erratum: Phys. Rev. D **107**, 119903 (2023)], arXiv:2207.13371 [hep-ph].
 - [5] R. Bause, H. Gisbert, and G. Hiller, (2023), arXiv:2309.00075 [hep-ph].
 - [6] L. Allwicher, D. Becirevic, G. Piazza, S. Rosauro-Alcaraz, and O. Sumensari, (2023), arXiv:2309.02246 [hep-ph].
 - [7] P. Athron, R. Martinez, and C. Sierra, (2023), arXiv:2308.13426 [hep-ph].
 - [8] T. Felkl, A. Giri, R. Mohanta, and M. A. Schmidt, (2023), arXiv:2309.02940 [hep-ph].
 - [9] X.-G. He, X.-D. Ma, and G. Valencia, (2023), arXiv:2309.12741 [hep-ph].
 - [10] C.-H. Chen and C.-W. Chiang, (2023), arXiv:2309.12904 [hep-ph].
 - [11] F. Abudinén *et al.* (Belle-II), Phys. Rev. Lett. **127**, 181802 (2021), arXiv:2104.12624 [hep-ex].
 - [12] T. E. Browder, N. G. Deshpande, R. Mandal, and R. Sinha, Phys. Rev. D **104**, 053007 (2021), arXiv:2107.01080 [hep-ph].
 - [13] X. G. He and G. Valencia, Phys. Lett. B **821**, 136607 (2021), arXiv:2108.05033 [hep-ph].
 - [14] T. Felkl, S. L. Li, and M. A. Schmidt, JHEP **12**, 118 (2021), arXiv:2111.04327 [hep-ph].
 - [15] X.-G. He, X.-D. Ma, and G. Valencia, JHEP **03**, 037 (2023), arXiv:2209.05223 [hep-ph].
 - [16] M. Ovchynnikov, M. A. Schmidt, and T. Schwetz, (2023), arXiv:2306.09508 [hep-ph].
 - [17] P. Asadi, A. Bhattacharya, K. Fraser, S. Homiller, and A. Parikh, (2023), arXiv:2308.01340 [hep-ph].
 - [18] A. Datta, S. Kamali, and D. Marfatia, Phys. Lett. B **807**, 135579 (2020), arXiv:2005.08920 [hep-ph].
 - [19] B. Batell, N. Lange, D. McKeen, M. Pospelov, and A. Ritz, Phys. Rev. D **95**, 075003 (2017), arXiv:1606.04943 [hep-ph].
 - [20] A. Datta, J. L. Feng, S. Kamali, and J. Kumar, Phys. Rev. D **101**, 035010 (2020), arXiv:1908.08625 [hep-ph].
 - [21] J. Liu, N. McGinnis, C. E. M. Wagner, and X.-P. Wang, JHEP **04**, 197 (2020), arXiv:2001.06522 [hep-ph].
 - [22] A. Aguilar-Arevalo *et al.* (MiniBooNE), Phys. Rev. Lett. **121**, 221801 (2018), arXiv:1805.12028 [hep-ex].
 - [23] E. Bertuzzo, S. Jana, P. A. Machado, and R. Zukanovich Funchal, Phys. Rev. Lett. **121**, 241801 (2018), arXiv:1807.09877 [hep-ph].
 - [24] P. Ballett, S. Pascoli, and M. Ross-Lonergan, Phys. Rev. D **99**, 071701 (2019), arXiv:1808.02915 [hep-ph].
 - [25] C. A. Argüelles, M. Hostert, and Y.-D. Tsai, Phys. Rev. Lett. **123**, 261801 (2019), arXiv:1812.08768 [hep-ph].
 - [26] P. Vilain *et al.* (CHARM-II), Phys. Lett. B **335**, 246 (1994).
 - [27] E. Valencia *et al.* (MINERvA), Phys. Rev. D **100**, 092001 (2019), arXiv:1906.00111 [hep-ex].
 - [28] A. M. Abdullahi, J. Hoefken Zink, M. Hostert, D. Massaro,

- and S. Pascoli, (2023), arXiv:2308.02543 [hep-ph].
- [29] T. Aoyama *et al.*, Phys. Rept. **887**, 1 (2020), arXiv:2006.04822 [hep-ph].
- [30] D. P. Aguillard *et al.* (Muon g-2), (2023), arXiv:2308.06230 [hep-ex].
- [31] S. M. Barr and A. Zee, Phys. Rev. Lett. **65**, 21 (1990), [Erratum: Phys.Rev.Lett. 65, 2920 (1990)].
- [32] A. B. Balantekin, A. de Gouvea, and B. Kayser, Phys. Lett. B **789**, 488 (2019), arXiv:1808.10518 [hep-ph].
- [33] A. J. Buras, J. Girrbach-Noe, C. Niehoff, and D. M. Straub, JHEP **02**, 184 (2015), arXiv:1409.4557 [hep-ph].
- [34] J. Grygier *et al.* (Belle), Phys. Rev. D **96**, 091101 (2017), [Addendum: Phys.Rev.D 97, 099902 (2018)], arXiv:1702.03224 [hep-ex].
- [35] O. Lutz *et al.* (Belle), Phys. Rev. D **87**, 111103 (2013), arXiv:1303.3719 [hep-ex].
- [36] S. Jäger and J. Martin Camalich, JHEP **05**, 043 (2013), arXiv:1212.2263 [hep-ph].
- [37] R. Aaij *et al.* (LHCb), JHEP **05**, 159 (2013), arXiv:1304.3035 [hep-ex].
- [38] L. Reina, G. Ricciardi, and A. Soni, Phys. Rev. D **56**, 5805 (1997), arXiv:hep-ph/9706253 [hep-ph].
- [39] D. Dutta *et al.* (Belle), Phys. Rev. D **91**, 011101 (2015), arXiv:1411.7771 [hep-ex].
- [40] M. Beneke, C. Bobeth, and R. Szafron, Phys. Rev. Lett. **120**, 011801 (2018), arXiv:1708.09152 [hep-ph].
- [41] S. Neshatpour, T. Hurth, F. Mahmoudi, and D. Martinez Santos, Springer Proc. Phys. **292**, 11 (2023), arXiv:2210.07221 [hep-ph].
- [42] A. J. Buras, D. Buttazzo, J. Girrbach-Noe, and R. Knegjens, JHEP **11**, 033 (2015), arXiv:1503.02693 [hep-ph].
- [43] J. K. Ahn *et al.* (KOTO), Phys. Rev. Lett. **126**, 121801 (2021), arXiv:2012.07571 [hep-ex].
- [44] G. Buchalla, G. D'Ambrosio, and G. Isidori, Nucl. Phys. B **672**, 387 (2003), arXiv:hep-ph/0308008.
- [45] A. Alavi-Harati *et al.* (KTeV), Phys. Rev. Lett. **93**, 021805 (2004), arXiv:hep-ex/0309072.
- [46] R. L. Workman *et al.* (Particle Data Group), PTEP **2022**, 083C01 (2022).
- [47] G. Khoriauli (NA48/2), J. Phys. Conf. Ser. **800**, 012035 (2017).
- [48] L. Di Luzio, M. Kirk, A. Lenz, and T. Rauh, JHEP **12**, 009 (2019), arXiv:1909.11087 [hep-ph].
- [49] J. Brod and M. Gorbahn, Phys. Rev. Lett. **108**, 121801 (2012), arXiv:1108.2036 [hep-ph].
- [50] P. Ball and R. Zwicky, Phys. Rev. D **71**, 014015 (2005), arXiv:hep-ph/0406232 [hep-ph].
- [51] A. Bharucha, D. M. Straub, and R. Zwicky, JHEP **08**, 098 (2016), arXiv:1503.05534 [hep-ph].
- [52] W. J. Marciano and Z. Parsa, Phys. Rev. D **53**, R1 (1996).
- [53] A. Lenz, Int. J. Mod. Phys. **A30**, 1543005 (2015), [,63(2014)], arXiv:1405.3601 [hep-ph].
- [54] Y. Aoki *et al.* (Flavour Lattice Averaging Group (FLAG)), Eur. Phys. J. C **82**, 869 (2022), arXiv:2111.09849 [hep-lat].
- [55] E. Cortina Gil *et al.* (NA62), JHEP **06**, 093 (2021), arXiv:2103.15389 [hep-ex].
- [56] E. Cortina Gil *et al.* (NA62), JHEP **02**, 201 (2021), arXiv:2010.07644 [hep-ex].
- [57] D. Hanneke, S. Fogwell, and G. Gabrielse, Phys. Rev. Lett. **100**, 120801 (2008), arXiv:0801.1134 [physics.atom-ph].
- [58] R. H. Parker, C. Yu, W. Zhong, B. Estey, and H. Müller, Science **360**, 191 (2018), arXiv:1812.04130 [physics.atom-ph].
- [59] T. Aoyama, T. Kinoshita, and M. Nio, Atoms **7**, 28 (2019).
- [60] G. Bernardi *et al.*, Phys. Lett. B **203**, 332 (1988).
- [61] A. Vaitaitis *et al.* (NuTeV, E815), Phys. Rev. Lett. **83**, 4943 (1999), arXiv:hep-ex/9908011.
- [62] A. M. Cooper-Sarkar *et al.* (WA66), Phys. Lett. B **160**, 207 (1985).
- [63] E. Gallas *et al.* (FMMF), Phys. Rev. D **52**, 6 (1995).
- [64] P. Vilain *et al.* (CHARM II), Phys. Lett. B **343**, 453 (1995).
- [65] K. Abe *et al.* (T2K), Phys. Rev. D **100**, 052006 (2019), arXiv:1902.07598 [hep-ex].
- [66] E. Cortina Gil *et al.* (NA62), Phys. Lett. B **816**, 136259 (2021), arXiv:2101.12304 [hep-ex].
- [67] P. Abratenko *et al.* (MicroBooNE), (2023), arXiv:2310.07660 [hep-ex].
- [68] A. de Gouvêa and A. Kobach, Phys. Rev. D **93**, 033005 (2016), arXiv:1511.00683 [hep-ph].
- [69] M. Carena, I. Low, and C. E. M. Wagner, JHEP **08**, 060 (2012), arXiv:1206.1082 [hep-ph].
- [70] A. Crivellin, M. Hoferichter, and M. Procura, Phys. Rev. D **89**, 054021 (2014), arXiv:1312.4951 [hep-ph].
- [71] M. Hoferichter, J. Ruiz de Elvira, B. Kubis, and U.-G. Meißner, Phys. Rev. Lett. **115**, 092301 (2015), arXiv:1506.04142 [hep-ph].
- [72] P. Junnarkar and A. Walker-Loud, Phys. Rev. D **87**, 114510 (2013), arXiv:1301.1114 [hep-lat].
- [73] R. H. Helm, Phys. Rev. **104**, 1466 (1956).
- [74] H. Davoudiasl and W. J. Marciano, Phys. Rev. D **98**, 075011 (2018), arXiv:1806.10252 [hep-ph].
- [75] J. P. Leveille, Nucl. Phys. B **137**, 63 (1978).

$B \rightarrow K\nu\bar{\nu}$, MiniBooNE and muon $g - 2$ anomalies from a dark sector
Supplemental Material

Alakabha Datta, Danny Marfatia and Lopamudra Mukherjee

I. DECAY WIDTHS

We collect expressions for the relevant decay widths.

The decay width of S to e^+e^- is

$$\Gamma_{S \rightarrow e^+e^-} = \frac{\eta_d^2}{8\pi} \frac{m_e^2 m_S}{v^2} \left(1 - 4 \frac{m_e^2}{m_S^2}\right)^{3/2}, \quad (\text{S1})$$

while its decay width to all three light neutrinos is

$$\Gamma_{S \rightarrow \nu\nu} = \frac{g_D^2}{8\pi} (1 - |U_{D4}|^2)^2 m_S. \quad (\text{S2})$$

The decay width of the dark scalar to two photons is

$$\Gamma_{S \rightarrow \gamma\gamma} = \frac{\alpha_{\text{EM}}^2 m_S^3}{1024\pi^3} \left| \frac{4\pi}{\alpha_{\text{EM}}} \kappa + \sum_{f=u,c,t,d} \frac{6\eta_f}{v} Q_f^2 A_{1/2}(r_f) \right|^2, \quad (\text{S3})$$

where f denotes all spin 1/2 fermions with electric charge Q_f , and $r_f = 4m_f^2/m_S^2$. The loop function $A_{1/2}$ is given by [69]

$$A_{1/2}(x) = 2x^2[x^{-1} + (x^{-1} - 1)f(x^{-1})], \quad (\text{S4})$$

with $f(x) = \arcsin^2 \sqrt{x}$ for $m_S < 2m_f$.

The decay width of ν_4 to $S\nu$ (where ν denotes all three light neutrinos) is

$$\Gamma_{\nu_4 \rightarrow S\nu} = \frac{g_D^2}{8\pi} |U_{D4}|^2 (1 - |U_{D4}|^2) \left(1 - \frac{m_S^2}{m_{\nu_4}^2}\right)^2 m_{\nu_4}. \quad (\text{S5})$$

II. MESON DECAYS

The branching fractions for the different exclusive FCNC processes of interest are given by [20]

$$\mathcal{B}(B \rightarrow KS) = \frac{|g_{bs}|^2 f_0^2(m_S^2) \sqrt{\lambda(m_B^2, m_K^2, m_S^2)}}{64\pi m_B^3} \left(\frac{m_B^2 - m_K^2}{m_b - m_s}\right)^2 \tau_B, \quad (\text{S6})$$

$$\mathcal{B}(B \rightarrow K^*S) = \frac{|g_{bs}|^2 A_0^2(m_S^2) \lambda(m_K^2, m_\pi^2, m_S^2)^{3/2}}{64\pi m_B^3 (m_b + m_s)^2} \tau_B, \quad (\text{S7})$$

$$\mathcal{B}(K \rightarrow \pi S) = \frac{|g_{sd}|^2 f_{0,K}^2(m_S^2) \sqrt{\lambda(m_B^2, m_K^2, m_S^2)}}{64\pi m_K^3} \left(\frac{m_K^2 - m_\pi^2}{m_s - m_d}\right)^2 \tau_K, \quad (\text{S8})$$

$$\mathcal{B}(K_L \rightarrow \pi^0 S) = \frac{[\text{Re}(g_{sd})]^2 f_{0,K}^2(m_S^2) \sqrt{\lambda(m_{K^0}^2, m_{\pi^0}^2, m_S^2)}}{64\pi m_{K^0}^3} \left(\frac{m_{K^0}^2 - m_{\pi^0}^2}{m_s - m_d}\right)^2 \tau_{K_L}, \quad (\text{S9})$$

$$\mathcal{B}(K_S \rightarrow \pi^0 S) = \frac{[\text{Im}(g_{sd})]^2 f_{0,K}^2(m_S^2) \sqrt{\lambda(m_{K^0}^2, m_{\pi^0}^2, m_S^2)}}{64\pi m_{K^0}^3} \left(\frac{m_{K^0}^2 - m_{\pi^0}^2}{m_s - m_d}\right)^2 \tau_{K_S}, \quad (\text{S10})$$

where the kinematic function $\lambda(x, y, z) = x^2 + y^2 + z^2 - 2(xy + yz + zx)$ and $f_0(q^2)$, $A_0(q^2)$ are the relevant scalar B meson form factors [50, 51] while $f_{0,K}(q^2)$ is the kaon form factor [52].

The contributions to the branching ratio of the different B_s decays in the dark scalar model are given by [8, 20]

$$\mathcal{B}(B_s \rightarrow \gamma\gamma) = \frac{|g_{bs}|^2 \kappa^2}{64\pi} \frac{f_{B_s}^2 m_{B_s}^7}{m_b^2(m_{B_s}^2 - m_S^2)^2} \tau_{B_s}, \quad (\text{S11})$$

$$\mathcal{B}(B_s \rightarrow \mu^+ \mu^-) = \frac{|g_{bs}|^2 \eta_d^2 m_\mu^2}{32\pi v^2} \frac{f_{B_s}^2 m_{B_s}^5}{m_b^2(m_{B_s}^2 - m_S^2)^2} \left(1 - \frac{4m_\mu^2}{m_{B_s}^2}\right)^{3/2} \tau_{B_s}, \quad (\text{S12})$$

$$\mathcal{B}(B_s \rightarrow \nu\bar{\nu}) = \frac{|g_{bs}|^2 g_D^2 (1 - |U_{\mu 4}|^2)^2}{128\pi} \frac{f_{B_s}^2 m_{B_s}^5}{m_b^2(m_{B_s}^2 - m_S^2)^2} \left(1 - \frac{4m_{\nu 4}^2}{m_{B_s}^2}\right)^{3/2} \tau_{B_s}, \quad (\text{S13})$$

where f_{B_s} is the B_s meson decay constant [54].

III. MESON MIXING

The scalar contribution to B_s^0 mixing is given by [20]

$$\Delta M_{B_s} = -\frac{5}{12} \frac{|g_{bs}|^2}{m_{B_s}^2 - m_S^2} f_{B_s}^2 m_{B_s}. \quad (\text{S14})$$

A similar expression applies for kaon mixing.

IV. COHERENT SCATTERING

The interaction of the dark scalar to a nucleus with atomic number Z and mass number A is given by

$$\mathcal{L}_{SN} = C_N \bar{\psi}_N \psi_N S, \quad (\text{S15})$$

where ψ_N is the spinor of the nucleus and the effective coupling C_N in terms of the scalar coupling to protons (C_p) and neutrons (C_n) reads

$$C_N = ZC_p + (A - Z)C_n. \quad (\text{S16})$$

The proton and neutron couplings are related to the quark-scalar couplings by

$$C_p = \frac{m_p}{v} \left(\eta_c f_c^p + \eta_t f_t^p + \sum_d \eta_d f_d^p \right), \quad C_n = \frac{m_n}{v} \left(\eta_c f_c^n + \eta_t f_t^n + \sum_d \eta_d f_d^n \right), \quad (\text{S17})$$

where $m_p = 938.3$ MeV, $m_n = 939.6$ MeV are the proton and neutron masses and $f^{p,n}$ are the respective form factors [70–72].

The differential cross section of the coherent scattering process, $\nu_\mu + N \rightarrow \nu_4 + N$, is given by

$$\frac{d\sigma_S}{dT} = \frac{g_D^2}{16\pi} |U_{\mu 4} C_N|^2 (1 - |U_{\mu 4}|^2)^2 \frac{(2M + T)(m_{\nu 4}^2 + 2MT)}{E_{\nu_\mu}^2 (m_S^2 + 2MT)^2} F^2(T), \quad (\text{S18})$$

where E_{ν_μ} is the muon neutrino energy, M is the mass of the nucleus, T is the recoil energy, and $F(T)$ is the nuclear form factor [73].

V. $(g - 2)_\ell$

The dominant scalar contribution to $(g - 2)_\ell$ via the Barr-Zee diagram is given by [74]

$$\delta(g - 2)_\ell^{S\gamma\gamma} \approx \frac{\eta_d}{4\pi^2} \frac{\kappa m_\ell^2}{v} \ln \frac{\Lambda}{m_S}, \quad (\text{S19})$$

where Λ is the cutoff scale of the theory that generates the effective $S\gamma\gamma$ coupling.

The subdominant contribution from the one-loop correction is given by [75]

$$\delta(g - 2)_\ell^{(1\text{-loop})} = \frac{\eta_d^2}{8\pi^2} \frac{m_\ell^2}{v^2} \int_0^1 dz \frac{(1+z)(1-z)^2}{(1-z)^2 + z/r_\ell^2}, \quad (\text{S20})$$

where $r_\ell = m_\ell/m_S$.